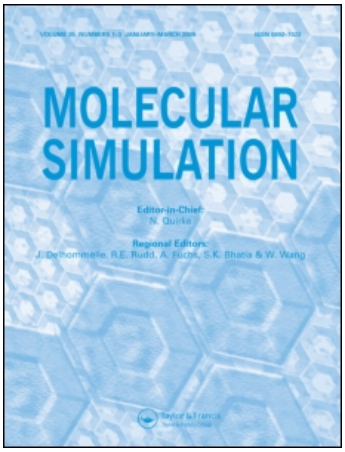

Molecular Simulation
Publication details, including instructions for authors and subscription information:
http://www.informaworld.com/smpp/title~content=t713644482

Quantum chemical insight on vibration spectra of silica systems

V. D. Khavryuchenko[a]; O. V. Khavryuchenko[b]; V. V. Lisnyak[b]
[a] Institute for Sorption and Problems of Endoecology, National Academy of Sciences of Ukraine, Kyiv, Ukraine [b] Kyiv National Taras Shevchenko University, Kyiv, Ukraine

To cite this Article Khavryuchenko, V. D. , Khavryuchenko, O. V. and Lisnyak, V. V.(2007) 'Quantum chemical insight on vibration spectra of silica systems', Molecular Simulation, 33: 6, 531 — 540
To link to this Article: DOI: 10.1080/08927020701203730
URL: http://dx.doi.org/10.1080/08927020701203730

Molecular Simulation, Vol. 33, No. 6, May 2007, 531–540

Taylor & Francis
Taylor & Francis Group

Quantum chemical insight on vibration spectra of silica systems

V. D. KHAVRYUCHENKO†§, O. V. KHAVRYUCHENKO‡* and V. V. LISNYAK¶‖

†Institute for Sorption and Problems of Endoecology, National Academy of Sciences of Ukraine, Gen. Naumova Street 13, 03680 Kyiv, Ukraine
‡Kyiv National Taras Shevchenko University, Volodymyrska Street 64, 01033 Kyiv, Ukraine
¶Kyiv National Taras Shevchenko University, Volodymyrska Street 64, 01033 Kyiv, Ukraine

(Received August 2006; in final form November 2006)

A set of silicate ions and corresponding lithium salts have been quantum chemically (QC) simulated in a "free molecule" approach. The infrared (IR), inelastic neutron scattering (INS), and Raman spectra have been simulated and fitted to the experimentally registered ones. The complete assignment of the vibrational bands along with the intensities and potential energy distribution has been performed. The applicability of the traditionally used quasimolecule Si—O—Si model to the interpretation of bands near 440–480 cm^{-1} and so-called "Boson" peak near 50 cm^{-1} has been critically discussed.

Keywords: Silica; Quantum chemical simulation (QC); Infrared spectra (IR); Inelastic neutron scattering (INS); Raman spectra; Boson peak

1. Introduction

Nowadays the production of silica optic fibres requires cheap and express ways to check the fitness of new technologies used. Since direct X-ray crystallography methods are not sufficient for completely amorphous solids, infrared (IR) and Raman spectroscopy are among the best methods of analysis. Using these methods, one can bind several bands in the spectra with structural characteristics of silica samples, i.e. the degree of crystallinity, concentration and distribution of structural defects including so-called "oxygen defects" and admixtures.

The aim of present work was to evaluate an adequate model for interpreting basic silica spectra features and to check the correctness of traditionally used models: the quasi-molecular Si—O—Si model [1–8], the small cluster models [9–11] and the soft potential-based solid state model [12] (the vibration analysis of all these models has been performed in the Cartesian coordinates).

Also, simulation of the spatial structure and vibrational properties of silica-based materials earlier has been performed at high level of approximation by density functional theory (DFT) and Car-Parinello methods in [13]. Unfortunately, these works have the same drawback, i.e. the analysis of vibrations is perfomed in the Cartesian coordinates, which, in some cases, may lead to somewhat incorrect assignment of the vibrations. The vibrations of certain types of atoms can be described in the framework of this method only, and interpretation of the data is quite debatable. In order to interpret correctly inelastic neutron scattering (INS), IR and Raman spectra of different silicas and silica-based glasses, an assignment in the internal coordinates is required, in other words the vibrational modes should be assigned in mathematically proved way. For that purpose the software for quantum chemical (QC) calculation and vibration spectra verification has been developed [14,15]. This software is adapted in particular for the glasses and cluster models. Also an example of successful combination of computational and spectral data during investigation of complicated systems has been given in the present study.

The QC modeling has been used to assign vibration bands of silica. In current paper we concentrated on small molecular models, used as a base for interpretation of IR, Raman and INS spectra of silica-based materials and simulated silica clusters up to 500 atoms [16–19]. The simulated vibration structure of big silica clusters posses from 500 to 1800 modes, which originate from modes of smaller silica species. So, it is reasonable to extrapolate

*Corresponding author. Tel.: + 380-44-2393306. Email: alexk@univ.kiev.ua
§Email: vkhavr@compchem.kiev.ua
‖Tel.: +380-44-2393306. Fax: +380-44-2581241. Email: lisnyak@univ.kiev.ua

Molecular Simulation
ISSN 0892-7022 print/ISSN 1029-0435 online © 2007 Taylor & Francis
http://www.tandf.co.uk/journals
DOI: 10.1080/08927020701203730

knowledge and characteristics of vibrational structure of small molecular models to larger silica clusters. The application of the DFT and Car-Parrinello approaches to systems larger than 300 atoms seems to be unrealistically time-consuming at the present computational state-of-art and may give erroneous results. Therefore, a semiempirical PM3 method [20] has been chosen to perform QC calculations.

The PM3 method has one significant drawback. The $I(\nu^{as}_{Si-O})/I(\delta_{O-SiO-O})$ relation in the PM3 method is 0.265, whereas for the AM1 QC method the same relation is 2.52. The origin of this phenomenon lays in the incorrect parameters for the core repulsion function [21]. Nevertheless, the PM3 is recommended, since only this method has some important features for the silica compounds and clusters calculation [22].

It is necessary to underline that simultaneous usage of different vibrational spectra recording techniques (INS, IR and Raman) is required to solve the problem of assignment correctly. IR and Raman spectroscopy are commonly used as complementary methods, since some normal vibrations are of zero intensity. However, all normal vibrations are active in the INS spectrum. The intensity of low frequency vibrations (below $300\,cm^{-1}$) is higher for the INS spectrum. From our experience [16–19], this situation is typical for all silicas and silica-based materials. Therefore, the INS spectroscopy is the best for the study of low frequency region, where librations with low IR and Raman intensity are situated. It should be kept in mind that resolving power of typical INS time-of-flight spectrometers (for instance KDSOG and NERA in JINR, Dubna, Russia; TOSCA in RAL, UK) is better for the low frequencies. But the INS spectra investigations require a lot of sample (sometimes for NERA up to 465 g of graphite was used for a good signal-to-noise merit). The INS spectra have low signal resolution and are observed as amplitude weighted density of states (AWDS). For ion-covalent object the INS spectra appear as smoothed and slightly disturbed plateau without sharp individual bands and have to be analyzed as a distribution function.

2. Experimental

2.1 Materials

Quartz glass was produced by Alcatel, France. Commercial fumed silica was supported by Wacker Chemie GmbH, Germany. The fumed silica samples were heated on at 1273 K for 6 h and then cooled to room temperature in air to purify from absorbed organic impurities.

2.2 Methods

The INS spectra for the quartz glass were measured in the frequency range of $10-10000\,cm^{-1}$ using inverted geometry time-of-flight spectrometers (KDSOG and NERA), installed in an IBR-2 nuclear pulse reactor at the Joint Institute for Nuclear Research (JINR) Dubna, Russia [23]. All spectra were recorded at 10 K to reduce the Debye–Waller factor. The pyrolytic graphite analyser with a resolution of *ca.* 2–3% $\Delta E/E$ (NERA) or 4–8% $\Delta E/E$ (KDSOG) has been used. Known weights (*ca.* 185 g) of finely ground samples were evenly loaded into aluminium foil sachets and mounted onto a centrestick, which was placed in a closed-cycle refrigerator in the instrument. The samples were then left to cool to 10 K and the spectra were recorded.

The diffuse reflections IR Fourier transformed spectra of the fumed silica, previously heated and dried at 1273 K, were recorded on a Nicolette 320X FTIR spectrometer. The spectral resolution was typically $4\,cm^{-1}$.

Jobin Yvon T64000 microspectrometer operating with argon ion laser (the wavelength of exciting beam is 514.5 nm, the spectral resolution is $1-0.3\,cm^{-1}$) and equipped for signal detection with a back-illuminated nitrogen-cooled Spex CCD matrix was used for the silica glass spectra recording. This instrument had a triple holographic monochromator as a filter. The laser spot diameter was about 3–5 μm for the micro-Raman measurements in backscattering configuration with 50 × ultra long focus Olympus MSPlan objective (numerical aperture = 0.80). The total magnification was 10, 50 and 100 × . Typical recording conditions in the low wave number region are 1800–3600 s.

The experimental spectra have been used to solve the inverted vibration problem for the QC simulated anions, since the anions are structural units of the soft matter, i.e. the quartz glasses or the fumed silica (considered next).

3. Methodology of QC calculation

Our computation software for silica cluster simulation and verification consists of two parts: the QuChem quantum chemistry program and the COSPECO vibration spectroscopy program [14,15]. Semiempirical and *ab initio* methods can be used to evaluate initial data for computational vibrational spectroscopy. Below semiempirical methods will be pointed only but the main features are also applicable to the *ab initio* results. The first step of the QC calculation is a local minimum optimisation since the potential function expansion and its approximation by the square-law function requires that the linear part of this expansion must be zero. Therefore, the experimental structure data should be optimised before a force field evaluation. After that the second derivatives matrix of the system's total energy respect to the atomic deviations is computed. The three points finite difference method has been used to compute the Cartesian force field matrix. The force field matrix has been divided into two parts referring to external and internal deformations coordinates [24] in order to avoid all errors resulting from the limited length of the floating point calculations and to keep the Eckart conditions.

The finite difference method also has been used to compute initial data for the IR and Raman spectra intensity.

But in contrast to the force field evaluation, the step size had to be increased from 0.003 to 0.1 Å due to low sensitivity of the total dipole moment to the small deviation of the atoms. The external electric field derivatives of polarizability have been computed by the finite difference method [25]. All results of the QC calculations have been obtained in the Cartesian coordinates, but normal coordinate analysis has been performed in the redundant internal coordinates. In order to do this, the force field has been transformed from the Cartesian to the internal redundant coordinate system.

The force field matrix in the Cartesian coordinates has been taken form the PM3 calculated model. In order to consider the Eckart conditions the matrix was projected onto independent coordinate system [24] and, thus, divided into the external and internal deformation coordinates. The internal part of the matrix has been considered for the computation of the vibrational spectra only.

Following formula was generated using standard notation for the **GF** method of Wilson–Deshius–Cross [26]

$$\mathbf{F} = \mathbf{G}^{-1}\mathbf{B}\mathbf{M}^{-1}\tilde{\mathbf{B}}(\mathbf{B}\tilde{\mathbf{B}})^{-1}\mathbf{B}\mathbf{U}^{\mathrm{mw}}\tilde{\mathbf{B}}(\mathbf{B}\tilde{\mathbf{B}})^{-1}\mathbf{B}\mathbf{M}^{-1}\tilde{\mathbf{B}}\mathbf{G}^{-1} \tag{1}$$

where $\mathbf{F}$ is the force constant matrix, $\mathbf{G}^{-1}$ is the inverted kinematics matrix, $\mathbf{B}$ and $\tilde{\boldsymbol{B}}$ and are the direct and transposed matrixes of conversion from the Cartesian to the internal coordinates, $\mathbf{U}^{\mathrm{mw}}$ is the mass-weighted Cartesian force matrix, $\mathbf{M}^{-1}$ is the inverted non-zero diagonal matrix of atomic masses, taken in triplicate, as $m_{11} = m_{22} = m_{33}$; $m_{44} = m_{55} = m_{66}$; ....

The pseudoinversion of kinematics matrix $\mathbf{G}$ has been used in order to make possible the inversion of the degenerated matrix $\mathbf{\Lambda}$ and to decrease numerical errors, associated with the inversion:

$$\mathbf{G}^{-1} = \mathbf{L}_{\mathbf{g}}\mathbf{\Lambda}_{\mathbf{g}}^{-1}\tilde{\mathbf{L}}_{\mathbf{g}} \tag{2}$$

$$\mathbf{\Lambda}_{\mathbf{g}}^{-1} = \begin{cases} = 1/\lambda & \varepsilon \le \lambda \\ = 0 & \varepsilon \ge \lambda \end{cases}$$

where $\mathbf{L}_{\mathbf{g}}$ is the form (relative amplitude) of normal vibration and $\mathbf{\Lambda}_{\mathbf{g}}$ is the diagonal matrix of the eigenvalues λ, which represent the vibrational frequencies by formula $\nu_i = C\sqrt{\Lambda_i}$ (coefficient C depends on the unit system), and $\mathbf{\Lambda}_{\mathbf{g}}^{-1}$ is the inverted matrix $\mathbf{\Lambda}_{\mathbf{g}}$. The matrix elements of $\mathbf{\Lambda}_{\mathbf{g}}^{-1}$ are compared to the ε parameter and the elements smaller than ε are nulled. The value of the ε parameter is chosen, basing on the computing system, i.e. the length of the computing word, the accuracy of the computation, etc. The $1/\varepsilon$ was taken about $5\,\mathrm{cm}^{-1}$ in current work.

The IR intensities have been computed as the derivatives of dipole moments taken in the Cartesian coordinates so long as the system orientation is kept. The Raman intensities are computed from the polarizabilities derivatives matrix. In order to perform this the polarizability tensor 3*3 $\boldsymbol{\alpha}$ is computed by the finite-field method at the stationary point:

$$\boldsymbol{\alpha}_{i1} = [\mu_i(E,0,0) - \mu_i(-E,0,0)]/2\|E\| \tag{3}$$

$$\boldsymbol{\alpha}_{i2} = [\mu_i(0,E,0) - \mu_i(0,-E,0)]/2\|E\| \tag{4}$$

$$\boldsymbol{\alpha}_{i3} = [\mu_i(0,0,E) - \mu_i(0,0,-E)]/2\|E\| \tag{5}$$

where μ_i is the dipole moment component along i-axis, E is a vector of external electric field, $\boldsymbol{\alpha}_{ij}$ are the component of the polarizability tensor produced by differentiation of μ_i by E along j-axis. The matrix of the $\boldsymbol{\alpha}_{ij}$ dipole moments derivatives, i.e. polarizability tensor, is used to evaluate the polarizabilities derivatives matrix.

The detailed description of the vibrational spectra calculation method used was given in Ref. [15].

4. Results and discussion

4.1 Systems description

Several variants have been considered when selecting the model of the silica prototype molecules. The model of the "saturated" H_4SiO_4 molecule, reported in Ref. [27] was found to be inapplicable due to high covalency of the O—H bond and high impact of the kinematic effect, which alters vibrational structure of the system drastically. Also, the IR, Raman and INS spectra of the H_4SiO_4 in molecular form cannot be found in scientific sources. Therefore, the model of "free" anions has been supposed to be more adequate. The Li silicates of corresponding ions have been simulated in order to consider the effect of counter-ions and to compensate an unrealistic charge distribution in the charged clusters (see section 4.2 for a more detailed discussion).

Several "free" anions and corresponding silicates in a "free one-molecule approach" have been used for examination. These anions with corresponding silicates in the "free one-molecule approach" have been studied in order of increasing complexity of the units. Calculated geometrical characteristics, charges and Wiberg indexes, i.e. the bond orders, for all QC simulated clusters are listed in table 1. The geometries, experimental and calculated spectra (with inverted vibration problem solved) of the SiO_4^{-4} and $Si_2O_7^{-6}$ anions are shown in figures 1 and 2, respectively. These data along with vibration modes assignment for other objects under study can be found in supplementary materials.

A set of silicate anions SiO_4^{-4}, $Si_2O_7^{-6}$, $Si_3O_9^{-6}$, $Si_4O_{12}^{-8}$ and $Si_8O_{20}^{-8}$ has been studied in order to examine the changing in the bands splitting upon the system growth. All of the systems have unrealistic charge distribution with negatively charged silicon atoms, too high values for HOMO and LUMO, negative ionisation potential and positive values of heats of formation. Due to this reason, as one can see from figure 1, the electron density of states (EDOS) function is shifted to the positive energy region with Fermi level (HOMO) determined around 12 eV (figure 1). In particular for QC calculated $Si_2O_7^{-6}$ anion,

Table 1. The QC derived parameters of the simulated clusters.

Cluster	*Heat of formation (kcal/mol)*	*Ionization potential (eV)*	*Charges on atoms*	*Wiberg indexes*	E_{HOMO} *(eV)*	E_{LUMO} *(eV)*
SiO_4^{-4}	443.48	−12.87	$q_{Si} = -0.1666$	$W_{Si-O} = 0.9905$	12.8714	24.3037
			$q_O = -0.9584$	$W_{O-O} = 0.0716$		
$Si_2O_7^{-6}$	840.72	−16.67	$q_{Si} = 0.0175$	$W_{Si-O} = 0.8113$	16.6654	25.5090
			$q_O = -0.3548$	$W_{Si-\bar{O}} = 1.0273$		
			$q_{\bar{O}} = -0.9452$	$W_{O-O} = 0.0740$		
Li_4SiO_4	−288.73	8.19	$q_{Si} = 0.9550$	$W_{Si-O} = 0.9118$	−8.1852	−0.2782
			$q_O = -0.5388$	$W_{O-O} = 0.0451$		
			$q_{Li} = 0.3000$	$W_{Li-O} = 1.1483$		
$Li_6Si_2O_7$	−530.88	7.40	$q_{Si} = 1.0206$	$W_{Si-O} = 0.8714$	−7.4032	−0.1411
			$q_O = -0.5320$	$W_{Si-\bar{O}} = 0.9075$		
			$q_{\bar{O}} = -0.5478$	$W_{O-O} = 0.0496$		
$Si_3O_9^{-6}$	496.07	−14.69	$q_{Si} = 0.2695$	$W_{Si-O} = 0.8430$	14.6866	24.0818
			$q_O = -0.4098$	$W_{Si-\bar{O}} = 1.0844$		
			$q_{\bar{O}} = -0.9300$	$W_{O-O} = 0.0542$		
$Li_6Si_3O_9$	−751.067	7.30	$q_{Si} = 1.0537$	$W_{Si-O} = 0.8649$	−7.2960	−0.0180
			$q_O = -0.5521$	$W_{Si-\bar{O}} = 0.9195$		
			$q_{\bar{O}} = -0.5607$	$W_{O-O} = 0.0410$		
			$q_{Li}^{+} = 0.3098$	$W_{Li-O} = 1.1346$		
$Si_4O_{12}^{-8}$	1089.67	−19.11	$q_{Si} = 0.2821$	$W_{Si-O} = 0.8426$	19.1129	28.3641
			$q_O = -0.3927$	$W_{Si-\bar{O}} = 1.0696$		
			$q_{\bar{O}} = -0.9448$	$W_{O-O} = 0.0632$		
$Li_8Si_4O_{12}$	−991.87	6.87	$q_{Si} = 1.0926$	$W_{Si-O} = 0.9070$	−6.8701	0.1433
			$q_O = -0.5634$	$W_{Si-\bar{O}} = 0.9048$		
			$q_{\bar{O}} = -0.5586$	$W_{O-O} = 0.0555$		
			$q_{Li}^{+} = 0.2968$	$W_{Li-O} = 1.1513$		
$Si_8O_{20}^{-8}$	−105.40	−15.35	$q_{Si} = 0.6402$	$W_{Si-O} = 0.8605$	15.3538	25.2908
			$q_O = -0.4796$	$W_{Si-\bar{O}} = 1.1415$		
			$q_{\bar{O}} = -0.9211$	$W_{O-O} = 0.0613$		
$Li_8Si_8O_{20}$	−1885.88	6.62	$q_{Si} = 1.1894$	$W_{Si-O} = 0.8499$	−6.6218	0.3543
			$q_O = -0.6175$	$W_{Si-\bar{O}} = 0.9257$		
			$q_{\bar{O}} = -0.5770$	$W_{O-O} = 0.0529$		
			$q_{Li}^{+} = 0.3135$	$W_{Li-O} = 1.1332$		

abnormally high charge on the one-coordinated oxygens ($-0.94524\ e^-$ in comparison with bridge oxygen charge of $-0.35479\ e^-$), and relatively close distance between these oxygens lead to high electrostatic Coulomb repulsion, and, consequently, to the distortion of the Si—O—Si angle from the equilibrium value 149° up to 155°. This points on the electrostatic interactions and, therefore, on the high value of the force constant for the Si—O—Si angle deformation. Further, the systems starting from the $Si_3O_9^{-6}$ anion have normal positive charged silicon atoms and, therefore, more realistic charge distributions due to the decreasing of excess of total negative charge per silicon atom. Also, it is noteworthy that the $Si_8O_{20}^{-8}$ anion has an anomalously low heat of formation (refers to table 1), i.e. the system is more thermodynamically stable than smaller silicate anions.

The SiO_4^{-4} anion has been examined numerously, including vibration analysis [28,29], but it is necessary to start the examination from this simplest unit for all silica-based materials studied. Fitted along with experimental data of [28,29], the INS, IR and Raman vibration spectra of SiO_4^{-4} are shown in the figure 1. One could observe a better agreement between calculated data and the experimental INS spectra plotted in figure 1.

In order to consider the effect of counter-ions, the lithium (Li_4SiO_4, $Li_6Si_2O_7$) and calcium ($Ca_3[Si_3O_9]$) silicates have been studied in the "free-molecule" approach. The presence of counter-ions does not disturb significantly the geometry of silicate ions. Still these molecules are neutral and, therefore, have appropriate charges on all atoms, values of the ionisation potential (table 1) and energies of the HOMO and LUMO in comparison with reference material, i.e. pure silica with $E_{HOMO} \cong -10.4$ eV and $E_{LUMO} \cong -1.2$ eV, found in Ref. [30].

Refers to geometry, the QC calculated lithium orthosilicate Li_4SiO_4 molecule considered in the free-molecular approach is high symmetric (T_d) as the corresponding anion. For the QC calculated $Li_6Si_2O_7$ molecule, the value of ∠Si—O—Si is 148.9°, which is well coincident with the value experimentally determined for amorphous silica as 144° [31].

The inverted vibration problem has not been solved in the case of Li_4SiO_4 and $Li_6Si_2O_7$ due to lack of experimental data. IR and Raman spectra of $Ca_3[Si_3O_9]$ and $Pb_4[Si_4O_{12}]$ have been taken from Ref. [8].

4.2 Vibration bands analysis

4.2.1 Si—O stretch vibrations region. This simplest model of the free orthosilicate anion SiO_4^{-4} cannot completely describe the silicas' experimental spectra, however, reproduces main features of their vibration spectra (figure 1, table 2).

In the idealised tetrahedron the asymmetrical vibration (ν^{as}_{Si-O}) is triple degenerated, but in the solid state this degeneration is removed due to interaction between Si—O bonds in the Si—O—Si bridge, so one observes more

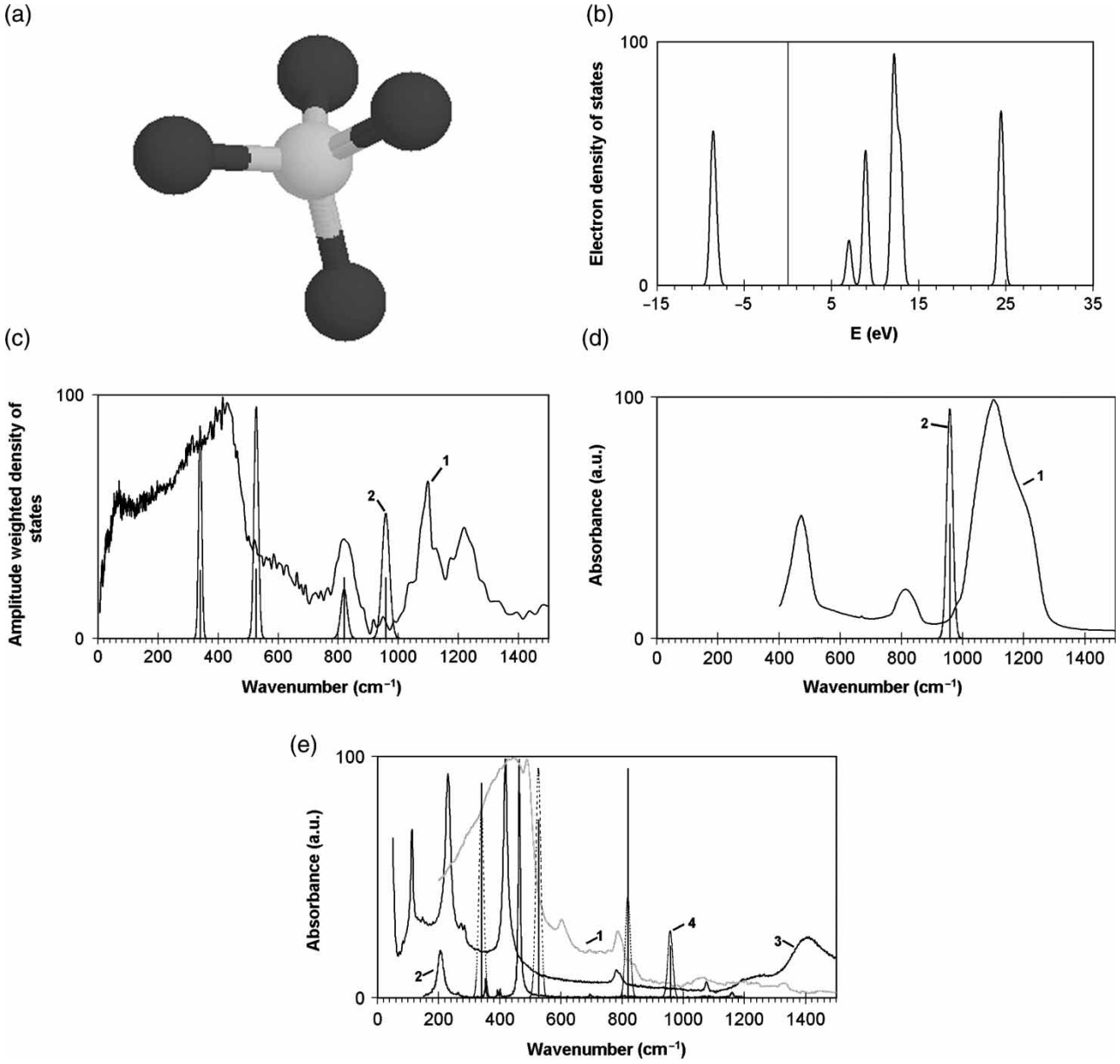

Figure 1. SiO_4^{-4}. (a) Computed structure. (b) EDOS electronic density of states. (c) INS spectra: (1) experimental INS of the pure silica glass; (2) and black lines QC calculated spectra. (d) IR spectra: (1) experimental IR of the pure silica; (2) and black lines QC calculated spectra. (e) Raman spectra: (1) experimental spectrum of the pure silica glass; (2) experimental spectrum of quartz; (3) experimental spectrum of cristobalite, dotted line; and (4) black sticks QC calculated spectra.

bands in the matrix vibrations region. The calculated vibration ν^{as}_{Si-O} at 957 cm^{-1} could be directly assigned to the mode in a range of 1000–1250 cm^{-1} registered experimentally. It is necessary to underline that literature data [29] shows that the ν^{as}_{Si-O} vibration in pure silicate ion differs significantly in the frequency from that of silica-based materials. The calculated symmetrical vibration ν^{sym}_{Si-O} at 820 cm^{-1} is close to the experimental value found at 818 cm^{-1}, since this vibration is pure by the form. Due to insignificant contribution of other vibrations the vibration slightly depends on the model's dimension.

The IR-intensity of orthosilicate anion SiO_4^{-4} is more sensitive to local surround. For pure silicate ion the ν^{sym}_{Si-O} vibration at 820 cm^{-1} is of zero intensity according to the selection rule. Therefore, experimentally observed bands at this position correspond to the interacting silicate ions but not to the isolated ones.

The $Si_2O_7^{-6}$ anion contains two bonded silicon–oxygen tetrahedrons with two types of interacting Si—O bonds (figure 2, table 3). This leads to the splitting of ν_{Si-O} vibrations. The highest vibration at 1013.15 cm^{-1} is assigned to the ν^{as}_{Si-O} vibration of the Si—O—Si bridge and the ν^{sym}_{Si-O} vibration of the Si—O—Si bridge is found at the 888.20 cm^{-1}. Interaction between the SiO_3 groups with local symmetry $C_{3\nu}$ and the Si—O—Si bridge leads to extra split of abovementioned vibrations. Therefore the distribution of the ν_{Si-O} vibrations is observed in the regions of 1000–1250 and 780–840 cm^{-1}. The same distribution is found for δ_{O-Si-O} vibrations, as it is shown below.

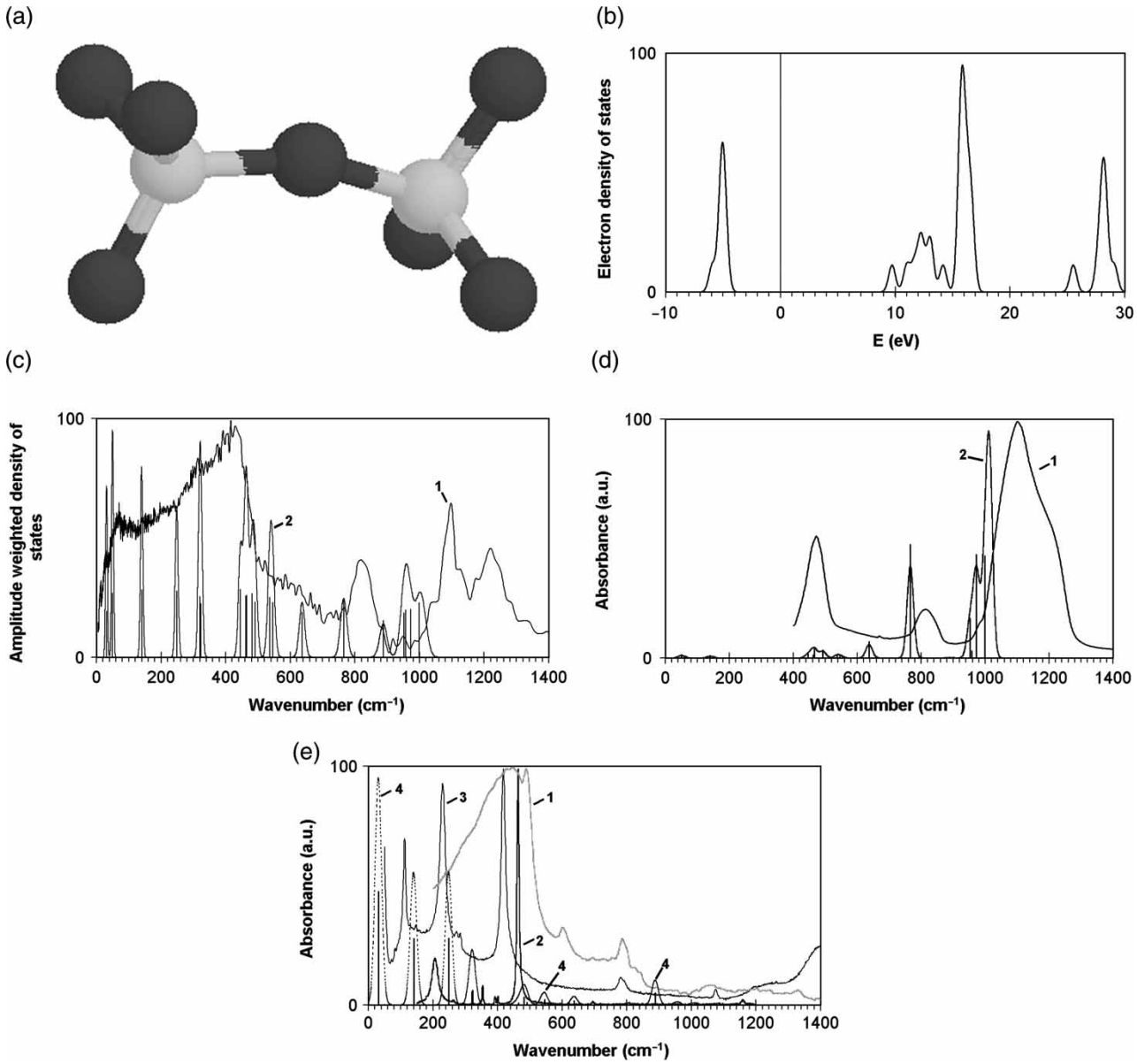

Figure 2. $Si_2O_7^{-6}$. (a) Computed structure. (b) EDOS, electronic density of states. (c) INS spectra: (1) experimental INS of the pure silica glass; and (2) black lines QC calculated spectra. (d) IR spectra: (1) experimental IR of the pure silica; and (2) black lines QC calculated spectra. (e) Raman spectra: (1) experimental spectrum of the pure silica glass; (2) experimental spectrum of quartz; (3) experimental spectrum of cristobalite, dotted line; and (4) black sticks QC calculated spectra.

Table 2. Vibration spectra of SiO_4^{-4} ion: frequencies, relative intensities, PED and bands assignment.

No.	*Frequency (cm^{-1})*	*INS relative intensity*	*IR relative intensity*	*Raman relative intensity*	*PED (%)*	*Assignment*
10	957.79	0.00	99.92	6.64	79.24	ν_{O-Si}
					20.76	δ_{O-Si-O}
9	957.68	87.95	100.00	9.12	79.21	ν_{O-Si}
					20.79	δ_{O-Si-O}
8	957.50	87.21	99.98	5.52	79.19	ν_{O-Si}
					20.81	δ_{O-Si-O}
7	818.99	87.14	0.00	11.10	100.00	ν_{O-Si}
6	526.45	87.92	0.27	58.20	43.97	ν_{O-Si}
					56.03	δ_{O-Si-O}
5	526.36	94.34	0.26	44.31	43.94	ν_{O-Si}
					56.06	δ_{O-Si-O}
4	526.29	100.00	0.27	52.13	43.91	ν_{O-Si}
					56.09	δ_{O-Si-O}
3	340.05	90.76	0.00	99.72	100.00	δ_{O-Si-O}
2	339.95	96.28	0.00	100.00	100.00	δ_{O-Si-O}

Table 3. Vibration spectra of $Si_2O_7^{-6}$ ion: frequencies, relative intensities, PED and bands assignment.

No.	*Frequency (cm^{-1})*	*INS relative intensity*	*IR relative intensity*	*Raman relative intensity*	*PED (%)*	*Assignment*
23	1013.15	56.66	100.00	6.83	19.08	ν_{O-Si}
					71.88	ν^{bridge}_{Si-O}
					5.24	δ_{O-Si-O}
22	998.42	80.60	42.46	3.66	73.45	ν_{O-Si}
					11.61	δ^{bridge}_{O-Si-O}
					7.16	δ_{O-Si-O}
21	972.45	70.78	42.95	1.29	82.32	ν_{O-Si}
					9.42	δ^{bridge}_{O-Si-O}
					7.49	δ_{O-Si-O}
20	957.69	69.70	2.98	6.91	86.77	ν_{O-Si}
					5.16	δ^{bridge}_{O-Si-O}
					7.43	δ_{O-Si-O}
19	952.19	65.63	16.46	7.00	84.81	ν_{O-Si}
					5.15	δ^{bridge}_{O-Si-O}
					7.18	δ_{O-Si-O}
18	888.20	54.63	0.28	87.76	67.13	ν_{O-Si}
					16.49	ν^{bridge}_{Si-O}
					6.95	δ^{bridge}_{O-Si-O}
					9.40	δ_{O-Si-O}
17	765.60	83.73	47.20	2.24	68.79	ν_{O-Si}
					28.96	ν^{bridge}_{Si-O}
16	636.67	66.48	6.77	17.77	33.09	ν_{O-Si}
					14.18	ν^{bridge}_{Si-O}
					32.61	δ^{bridge}_{O-Si-O}
					18.76	$\delta_{Si-O-Si}$
15	545.20	80.77	0.60	69.95	25.17	ν_{O-Si}
					17.60	ν^{bridge}_{Si-O}
					26.45	δ^{bridge}_{O-Si-O}
					26.76	δ_{O-Si-O}
14	537.17	88.42	1.38	6.03	25.19	ν_{O-Si}
					57.33	δ^{bridge}_{O-Si-O}
					15.21	δ_{O-Si-O}
13	491.61	81.33	3.40	14.41	13.83	ν_{O-Si}
					24.33	δ^{bridge}_{O-Si-O}
					59.06	δ_{O-Si-O}
12	481.62	93.69	0.03	29.42	18.03	ν_{O-Si}
					78.83	δ_{O-Si-O}
11	465.26	91.22	3.81	11.82	10.01	ν_{O-Si}
					18.37	δ^{bridge}_{O-Si-O}
					68.32	δ_{O-Si-O}
10	462.11	90.33	1.21	1.81	5.41	ν_{O-Si}
					9.91	δ^{bridge}_{O-Si-O}
					82.86	δ_{O-Si-O}
9	446.02	100.00	1.68	1.48	36.14	δ^{bridge}_{O-Si-O}
					61.73	δ_{O-Si-O}
8	322.97	78.96	0.07	26.16	84.58	δ^{bridge}_{O-Si-O}
					10.63	δ_{O-Si-O}
7	320.23	89.32	0.00	25.66	85.14	δ^{bridge}_{O-Si-O}
					11.49	δ_{O-Si-O}
6	248.66	97.40	0.08	100.00	33.47	ν^{bridge}_{Si-O}
					35.22	δ^{bridge}_{O-Si-O}
					31.01	δ_{O-Si-O}
5	140.05	99.37	0.98	44.44	70.87	$\delta_{Si-O-Si}$
4	49.92	94.77	1.34	0.05	98.32	χ^{asym}_{Si-O}
3	31.22	68.10	0.00	3.48	96.10	χ^{sym}_{Si-O}

One can observe rather high similarity in the region of 800–1200 cm^{-1}, if comparing the IR and Raman spectra of the lithium silicates Li_4SiO_4, $Li_6Si_2O_7$ and the corresponding anions. It means that lithium cation does not perturb the vibration spectrum of the main structural unit, i.e. SiO_4 tetrahedron.

4.2.2 Low-frequencies region. Two deformation vibrations δ_{O-Si-O} at 526 and 340 cm^{-1} in the SiO_4^{-4} anion calculated spectrum are shifted to the higher frequency region due to absence of interaction with other units of more complicate system and due to rather high Coulomb repulsion between negatively charged oxygen atoms. A very low intensity of the QC calculated δ_{O-Si-O} at 526 and 340 cm^{-1} bands can be explained by the imperfection of the PM3 QC method [21]. The QC calculated positions of previously mentioned normal vibrations coincide with the experiment better for the $Si_2O_7^{-6}$ anion in comparison with the SiO_4^{-4} one. Still, the overstated force constant of the Si—O—Si angle deformation (refers to section 4.1) leads to the shift of the corresponding QC computed modes to the high-frequencies region.

The noticeable participation of the $\delta_{Si-O-Si}$ vibration coordinates in the high frequency normal vibrations is observed (table 3). Potential energy distribution (PED) of the $\delta_{Si-O-Si}$ vibration coordinates for normal vibration at 636.67 cm^{-1} is 18.76%. But the maximal PED contribution of the $\delta_{Si-O-Si}$ vibration coordinates (70.87%) is observed for normal vibration at 140.05 cm^{-1} (table 3). Therefore, the $\delta_{Si-O-Si}$ vibration should be assigned to the low frequency region below 150 cm^{-1}, and this assignment is valid also for other silica-based compounds. Two lowest vibrations at 49.92 and 31.22 cm^{-1} are pure asymmetrical and symmetrical torsion vibrations along Si—O bond, correspondingly.

For this simple model of "free" disilicate $Si_2O_7^{-6}$ anion the $\delta_{Si-O-Si}$ and χ_{Si-O} normal vibrations are separated completely. But for more complicated silicas these two types of vibrations are mixed and observed as high vibration density of states from 5 up to 150 cm^{-1}. Depending on the local structure of the silicon–oxygen polyhedron, a part of the δ_{O-Si-O} vibrations may participate in the low frequencies vibrations. For the amorphous silicas [32–34] the amplitude of these normal vibrations increases and as the result so-called "Boson peak" is observed in the Raman and INS spectra. The phenomenon was not registered by IR-spectroscopy due to low dipole moment deviation of these vibrations.

So, the presented computations demonstrate that the "Boson peak" at 5–150 cm^{-1} should be interpreted as a sum of low-intensive complex bands, composed mainly of the $\delta_{Si-O-Si}$, χ_{Si-O} and $\delta_{Si-O-Si}$ normal vibrations. This result is in a good agreement with the conclusions, given in a review of Nakayama [35], where the "Boson peak" is assigned to the lowest transverse optic modes associated with the coupled rotational motions of the SiO_4 tetrahedra. However, the review cited, though giving an excellent experimental ground, presents a phenomenological model only, not supported by molecular simulations. Hence, the low-frequency vibrations in Ref. [35] are not associated with the $\delta_{Si-O-Si}$ and $\delta_{Si-O-Si}$ deformational modes, which makes notion about the nature of the "Boson peak" somewhat imperfect.

The phenomenon of the baseline growth in 150–400 cm^{-1} region is also explained by the computed models. The number of independent δ_{O-Si-O} vibrations (five for SiO_4 tetrahedron) is higher than number of the ν_{Si-O} vibrations (four for SiO_4 tetrahedron). These ν_{Si-O} vibrations strongly interact with the δ_{O-Si-O} vibrations. The value of this interaction (non-diagonal force constants) is comparable with diagonal force constants for the δ_{O-Si-O} vibrations, but is much less than force constants for the ν_{Si-O} vibrations. This factor leads to the broadening of the δ_{O-Si-O} vibrations region in Raman spectra upon complication of the systems. Therefore, the gap between δ_{O-Si-O} and $\delta_{Si-O-Si}$ vibrations with respective contribution of the χ_{Si-O} vibrations disappears. This also can be observed directly from the VDOS or INS spectra.

According to the selection rules, the IR and Raman intensity of the great number of the normal vibrations decreases for the perfect crystals and one can observe only several well-resolved narrow peaks. This effect is better displayed for the Raman spectra of quartz and cristobalite. The IR spectra for these silicas contain more broadening peaks with a near-zero intensity between them, while the INS spectra of these compounds have nonzero intensity between main peaks.

The QC simulated characteristics of the cyclic trisilicate anion $Si_3O_9^{-6}$ and more complicated silica anions are shown along with the experimental spectra in supplementary materials. In general their spectra have the same view as previously described, but upon the complication of the system the number of torsion and deformational vibrations grows much faster than the number of valent vibrations. This leads to the increasing of VDOS in the low-frequency region.

The $Si_3O_9^{-6}$ is a typical complicated system [22], so the $\delta_{Si-O-Si}$ vibration coordinates are distributed between many normal vibrations. The maximal contribution of these vibrations is observed into two normal vibrations at the 436 cm^{-1}. But even in this case this participation are only 17.70% of PED. It means that these normal vibrations could hardly be stated as ring vibrations and its assignment to the vibration of Si_3O_9 ring is problematical.

The QC simulated vibration spectra of the lithium silicates do not drastically differ from these of pure anions by frequencies. The frequencies coincide with a good accuracy (better than $\sim$20 cm^{-1}) but intensities are not reproduced with the sufficient accuracy. There is good reason to suppose that one can observe the influence of the cation on the electron density distribution changing. Since the silica ions are covalent, the cations are not able to change significantly the force constants but influence

mainly on the external electric field responsibility of the system under study, i.e. on the Raman spectra intensity.

The good coincidence by frequencies between the QC simulated and experimental IR spectra in the case of lithium silicates is explained by the correct charge distribution, which leads to more suitable force constants. Corresponding normal values for the $\delta_{Si-O-Si}$ and χ_{Si-O} vibrations are found at the 63.02, 43.27 and 34.67 cm^{-1}.

Summarising, one can conclude that the simple model of SiO_4^{-4} anion alone is inefficient in interpreting the spectra of silica and more complicated models should be used. But, in any case, this model can reproduce at least the number and position of the Raman bands in the experimental spectra for quartz and cristobalite.

Other non adequate model for vibration spectra interpretation of amorphous silica is the simplest triatomic model of the siloxane bridge Si—O—Si [1–8], which, however, does not exist as a free molecule.

The nearest related molecules are disiloxane $H_3Si—O—SiH_3$ and its/the disiloxane halogen-substituted analogues $Hal_3Si—O—SiHal_3$. For stated molecules the $\delta_{Si-O-Si}$ frequency is observed between 8–65 cm^{-1} [36,37] in contrast with the sophistic value calculated by the triatomic model (420–480 cm^{-1}) [1–8]. The origin of this difference is concerned with the fact that the Cartesian shift is used for assignment of the vibration modes in the quasi-molecule approach but not the form of the normal vibrations. Such interpretation gives incorrect assignments in the case of bridging oxygen atom vibrations. So, the calculation of the Si—O—Si angle directly from the position of the vibration band at 420–480 cm^{-1} is erroneous. The present study shows that the band at 420–480 cm^{-1} should be assigned to the δ_{O-Si-O} vibration mainly, i.e. up to 80–90% of the PED. Only 10–20% of this normal vibration PED belongs to the $\delta_{Si-O-Si}$ vibration.

In order to judge about correctness of the triatomic model application to silica vibrational spectra computation, the force field fitted for the disiloxane molecule $H_3Si—O—SiH_3$ was applied and vibration modes for the triatomic model were computed. The asymmetrical and symmetrical ν_{Si-O} bonds and the deformation vibrations $\delta_{Si-O-Si}$ at 1205.6, 680.6 and 46.6 cm^{-1} were determined, respectively. So, the number of the theoretical and experimentally observed bands is in a disagreement (as can be seen from the figure 1). The represented data confirms that the triatomic model using the Si—O—Si pseudo-molecule is non-adequate.

5. Conclusions

The INS, IR and Raman spectra of silica glass have been measured and compared with the literature data for the lithium or calcium salts of polysilcates. Analysing obtained set of all vibration frequencies calculated by QC methods for the small clusters in the "free-molecule" approach one can come to several conclusions. A popular but incomplete model of the silica like Si—O—Si quasi-molecule leads to the incorrect assignments for the main vibration bands, observed experimentally. The band at 440–480 cm^{-1} has been previously assigned to the $\delta_{Si-O-Si}$ vibration because this oversimplified model can proposed only three vibration modes.

However, the study of more sophisticated models with tetrahedral oxygen environment shows that the band in this region should be assigned to the δ_{O-Si-O} vibrations as well as for all typical tetrahedral molecules or ions. The incorrect assignment for the oversimplified model demands introducing of the "Boson" peak to describe the vibration bands near 150 cm^{-1}. Thus it can be marked that even the simple molecule containing Si—O—Si bridge has vibration at 50 cm^{-1}, which was unambiguously assigned to $\delta_{Si-O-Si}$ vibration.

Supplementary information for this paper can be found online at http://www.informaworld.com

References

[1] F.L. Galeener. Band limits and the vibrational spectra of tetrahedral glasses. *Phys. Rev. B.*, **19**, 4292 (1979).

[2] F.L. Galeener, A.E. Geissberger. Vibrational dynamics in 30Si-substituted vitreous SiO_2. *Phys. Rev. B*, **27**, 6199 (1983).

[3] F.L. Galeener, J.C. Mikkelsen Jr.. Vibrational dynamics in 18O-substituted vitreous SiO_2. *Phys. Rev. B*, **23**, 5527 (1981).

[4] E. Geissberger, F.L. Galeener. Raman studies of vitreous SiO_2 versus fictive temperature. *Phys. Rev. B*, **28**, 3266 (1983).

[5] R.A. Barrio, F.L. Galeener, E. Martfnez, R.J. Elliott. Regular ring dynamics in AX_2 tetrahedral glasses. *Phys. Rev. B*, **48**, 15672 (1983).

[6] M.F. Thorpe, F.L. Galeener. Network dynamics. *Phys. Rev. B*, **22**, 3078 (1980).

[7] R.A.B. Devine. Structural nature of the Si/SiO_2 interface through infrared spectroscopy. *Appl. Phys. Lett.*, **68**, 3108 (1996).

[8] M. Handke, M. Sitarz, W. Mozgawa. Model of silicooxygen ring vibrations. *J. Mol. Struct. (Theochem)*, **450**, 229 (1998).

[9] G. Pacchioni, M. Vitiello. Infra-red, electron paramagnetic resonance and X-ray photoemission spectral properties of point defects in silica from first-principle calculations. *J. Non-Cryst. Solids*, **245**, 175 (1999).

[10] G. Pacchioni, M. Vitiello. EPR and IR spectral properties of hydrogen-associated bulk and surface defects in SiO_2: *ab initio* calculations. *Phys. Rev. B*, **58**, 7745 (1998).

[11] J. Sarnthein, A. Pasquarello, R. Car. Origin of the high-frequency doublet in the vibrational spectrum of vitreous SiO_2. *Science*, **275**, 1925 (1997).

[12] C. Oligschleger. Dynamics of SiO_2 glasses. *Phys. Rev. B*, **60**, 3182 (1999).

[13] S. Ispas, N. Zotov, S. De Wispelaere, W. Kob. Vibrational properties of a sodium tetrasilicate glass: *ab initio* versus classical force fields. *J. Non-Cryst. Solids*, **351**, 1144 (2005).

[14] A.V. Khavryutchenko, V.D. Khavryutchenko. Quantum chemistry simulation of 60-fullerene: interaction under external pressure. *Z. Naturforsch. A*, **60**, 41 (2005).

[15] V. Khavryutchenko. Computation vibration spectroscopy as a tool for investigation of complicated systems. *Euras. ChemTech J.*, **6**, 157 (2004).

[16] V. Khavryutchenko, J. Garapon, B. Poumellec. Structure simulation of silica glasses: approach to CVD. *Modelling Simul. Mater. Sci. Eng.*, **9**, 465 (2001).

[17] E. Sheka, I. Natkaniec, V. Khavryutchenko, E. Nikitina, H. Barthel. INS study of intermolecular interaction at the silicone-fumed silica interface. *Physica B*, **276–278**, 244 (2000).

[18] E. Sheka, V. Khavryutchenko, I. Markichev. Technological polymorphism of disperse amorphous silicas: inelastic neutron scattering and computer modelling. *Russ. Chem. Rev.*, **64**, 419 (1995).

[19] E. Sheka, I. Natkaniec, V.D. Khavryutchenko, P. Nechitaylov, A. Muzychka, V. Ogenko, I. Markichev, J. Brankowski, J. Krawczyk. Vibrational spectroscopy of dispersed silica: inelastic neutron scattering. *J. Electron. Spectrosc. Relat. Phenom.*, **54/55**, 855 (1990).

[20] J.J.P. Stewart. Optimization of parameters for semiempirical methods II. Applications. *J. Comp. Chem.*, **10**, 221 (1989).

[21] G.I. Csonka, J.G. Angyan. The origin of the problems with PM3 core repulsion function. *J. Mol. Struct. (Theochem)*, **393**, 31 (1997).

[22] W.S. Verwoerd, K. Weimer. Comparison of semiempirical calculations for silicon compounds. *J. Comput. Chem.*, **12**, 417 (1991).

[23] I. Natkaniec, S.I. Bragin, J. Brankowski. *Proceedings of ICANS XII*, RAL Report No. 94–025, vol. I, pp. 89, Abingdon (1993).

[24] I.H. Williams. Force-constant computations in Cartesian coordinates. Elimination of translational and rotational contributions. *J. Mol. Struct.*, **94**, 275 (1983).

[25] E.F. Sheka, V.D. Khavryutchenko, V.A. Zayetz. Computer modeling of assembly of atoms in an electric field. *Int. J. Quant. Chem.*, **57**, 741 (1996).

[26] P.C. Painter, M.M. Coleman, J.L. Koenig. *The Theory of Vibrational Spectroscopy and its Application to Polymeric Materials*, p. 530, Wiley, New York, NY (1982).

[27] G.J. Kramer, N.P. Farragher, B.W.H. van Beest, R.A. van Santen. Interatomic force fields for silicas, aluminophosphates, and zeolites: derivation based on *ab initio* calculations. *Phys. Rev. B*, **43**, 5068 (1991).

[28] L.G. Alekhina, M.V. Akhmanova, V.A. Dementiev, L.A. Gribov. The solution of inverted spectroscopic problem for SiO_4-group (in Russian). *Zh. Prikl. Spektrosk., (J. Appl. Spectr.*, **22**, 720 (1975).

[29] K. Nakamoto. *Infrared and Raman Spectra of Inorganic and Coordination Compounds (Infrared and Raman Spectra of Inorganic and Coordination Compounds, Theory and Applications in Inorganic Chemistry)*, 4-ed., p. 408, Wiley Interscience, New York, NY (1997).

[30] D.L. Griscom. The electronic structure of SiO_2: a review of recent spectroscopic and theoretical advances. *J. Non-Cryst. Solids*, **24**, 155 (1977).

[31] H.F. Poulsen, H.-B. Neumann, J.R. Schneider, J. Neuefeind, M.D. Zeidler. Amorphous silica studied by high energy X-ray diffraction. *J. Non-Cryst. Solids*, **188**, 63 (1995).

[32] S.N. Taraskin, S.R. Elliott. Anharmonicity and localization of atomic vibrations in vitreous silica. *Phys. Rev. B*, **59**, 8572 (1999).

[33] U. Buchenau, M. Prager, N. Nucker, A.J. Dianoux, N. Ahmad, W.A. Phillips. Low-frequency modes in vitreous silica. *Phys. Rev. B*, **34**, 5665 (1986).

[34] A. Hehlen, E. Courtens, A. Yamanaka, K. Inoue. Nature of the Boson peak of silica glasses from hyper-Raman scattering. *J. Non-Cryst. Solids*, **307–310**, 87 (2002).

[35] T. Nakayama. Boson peak and terahertz frequency dynamics of vitreous silica. *Rep. Prog. Phys.*, **65**, 1195 (2002).

[36] J.R. Durig, M.J. Flanagan, V.F. Kalasinsky. Raman spectra of gases. XIV. Hexachlorodisiloxane. *J. Mol. Struct.*, **27**, 241 (1975).

[37] J.R. Durig, E.L. Varettl, W.J. Natter, A. Muller. Infrared spectrum of matrix-isolated hexachlorodisiloxane and low frequency Raman spectrum of the gas. *J. Mol. Struct.*, **49**, 43 (1978).